Simultaneous Measurement of Nonlinearity and Electrochemical Impedance for Protein Sensing Using Two-Tone Excitation

Jonathan S. Daniels, Erik P. Anderson, Thomas H. Lee, and Nader Pourmand

***Abstract*— Impedance biosensors detect the binding of a target to an immobilized probe by quantifying changes in the impedance of the electrode-electrolyte interface. The interface's I-V relationship is inherently nonlinear, varying with DC bias, and target binding can alter the degree of nonlinearity. We propose and demonstrate a method to simultaneously measure the nonlinearity and conventional small-signal impedance using intermodulation products from a two-tone input. Intermodulation amplitudes accurately reflect the impedance's manually-measured voltage dependence. We demonstrate that changes in nonlinearity can discriminate protein binding. Our measurements suggest that target binding can alter nonlinearity via the voltage dependence of the ionic double layer.**

I. Introduction

Impedance biosensors detect the binding of a target molecule to an immobilized probe by quantifying impedance changes of the electrode-electrolyte interface [1], [2]. Although this interface has a nonlinear current-to-voltage (I-V) characteristic, it is usually modeled with linear elements [2], [3]. In order to have a linear response, the measurement excitation must be small compared with the thermal voltage ($V_T \simeq 26\,\mathrm{mV}$) [4]. Although in some senses a limitation, the nonlinearity of the biofunctionalized interface can be exploited as a sensed variable along with the small-signal impedance.

In electrochemical impedance spectroscopy (EIS), the magnitude and phase of the electrode-electrolyte interface impedance are measured at various frequencies and the data is subsequently fit to a circuit model to extract values such as the charge transfer resistance and surface capacitance [2]. The impedance depends on the DC bias. To measure the impedance as both a function of frequency and bias, it is possible to repeat the frequency sweep at various bias voltages at the expense of extra measurement time [5].

We propose and demonstrate a method for quantifying the impedance's dependence on bias voltage by superposing a second excitation tone which varies the DC bias. The amount of nonlinearity is encoded in the magnitude of the resulting intermodulation tones, with no extra measurement time.

As a simplified illustration, consider measuring the capacitance of the ionic double layer, which is voltage-dependent. The Gouy-Chapman theory predicts the capacitance of a monovalent 1:1 electrolyte (e.g. NaCl) on a bare electrode is

$$C_{dl}(\phi) = \left(228\,\mu\mathrm{F/cm}^2\right)\sqrt{\frac{C_0}{\mathrm{mol/L}}}\left(1+\frac{1}{8}\left(\frac{\phi}{V_T}\right)^2\right) \quad (1)$$

where C_0 is the bulk concentration, ϕ is the surface potential relative to the potential of zero charge (PZC), and the series expansion for hyperbolic cosine has been truncated after the quadratic term (see Section 13.3.2 of [3]). To measure C_{dl} we must impose a nonzero excitation voltage ϕ, which in turn changes the value of C_{dl}. If a $50\,\mathrm{mV}$ amplitude tone at f_0 is used, C_{dl} changes by about 50% during the measurement. This generates a tone at $3f_0$ with amplitude of about 10% relative to the f_0 tone. Hence, measuring harmonics of f_0 can lead to information about the voltage dependence of the impedance. This measurement approach has been sparingly used in biosensors to date [6]. One practical difficulty is that the harmonic tones are widely spaced.

In contrast with the example above, our method utilizes two excitation tones to simultaneously measure the impedance and nonlinearity of the device under test (DUT); in our case, the DUT is the biofunctionalized electrode-electrolyte interface. The DUT's nonlinear I-V characteristic generates intermodulation (IM) products. We use an input excitation

$$V_{in} = A\cos(\omega_A t) + B\cos(\omega_B t) \quad (2)$$

where the two tones are:

1) a swept-frequency tone at frequency ω_A, amplitude $A \ll V_T$ (to measure the small-signal impedance)
2) a fixed low-frequency tone at frequency ω_B, amplitude $B \gg A$ (to vary the effective DC bias)

We approximate the nonlinear DUT impedance as

$$Z_{DUT}(\omega) = Z_0(\omega)\left(1+\alpha_1 V_{in}+\alpha_2 V_{in}^2\right) \quad (3)$$

where $Z_0(\omega)$ is the small-signal impedance and α_1 and α_2 encode the bias dependence (for notational simplicity, we ignore the fact that α_1 and α_2 depend on frequency). For our transimpedance measurement circuit (Fig. 1), the transfer function is $-Z_f(\omega)/Z_{DUT}(\omega)$. Then

$$V_{out} = -V_{in}\frac{Z_f(\omega)}{Z_0(\omega)}\frac{1}{1+\alpha_1 V_{in}+\alpha_2 V_{in}^2}. \quad (4)$$

If the nonlinearity is relatively small — $|\alpha_1 V_{in}| \ll 1$ and $\left|\alpha_2 V_{in}^2\right| \ll 1$ — we can rewrite the denominator using

This work supported in part by the National Human Genome Research Institute (HG000205/HG/NHGRI and T32 HG00044/HG/NHGRI) and the National Science Foundation (DBI-0551990).

J. S. Daniels, E. P. Anderson, and N. Pourmand are with the Stanford Genome Technology Center, Stanford University Dept. of Biochemistry. N. Pourmand is also with Dept. of Biomolecular Engineering, University of California Santa Cruz. Email: pourmand@soe.ucsc.edu.

J. S. Daniels, E. P. Anderson, and T. H. Lee are with the Stanford Center for Integrated Systems, Stanford University Dept. of Electrical Engineering. Email: jon.daniels@stanford.edu.

$(1+\delta)^{-1} \simeq 1-\delta$. It follows, using trigonometric identities, that the output tones near ω_A are given by[1]

$$\begin{aligned} V_{out} &= \tfrac{-Z_f(\omega_A)}{Z_0(\omega_A)} A\cos(\omega_A t) \\ &+ \tfrac{1}{2}\alpha_1 AB \tfrac{Z_f(\omega_A-\omega_B)}{Z_0(\omega_A-\omega_B)} \cos((\omega_A-\omega_B)t) \\ &+ \tfrac{1}{2}\alpha_1 AB \tfrac{Z_f(\omega_A+\omega_B)}{Z_0(\omega_A+\omega_B)} \cos((\omega_A+\omega_B)t) \\ &+ \tfrac{1}{4}\alpha_2 AB^2 \tfrac{Z_f(\omega_A-2\omega_B)}{Z_0(\omega_A-2\omega_B)} \cos((\omega_A-2\omega_B)t) \\ &+ \tfrac{1}{4}\alpha_2 AB^2 \tfrac{Z_f(\omega_A+2\omega_B)}{Z_0(\omega_A+2\omega_B)} \cos((\omega_A+2\omega_B)t) \\ &+ \text{other terms far removed from } \omega_A \end{aligned} \quad (5)$$

where A, B, and $Z_f(\omega)$ are known or measurable. Note that the conventional impedance (Z_0) as well as the linear (α_1) and quadratic (α_2) terms of its voltage dependence can be quantified in a single two-tone experiment simply by measuring the tone amplitudes at $\omega_A \pm n\omega_B$ for $n = -2 \ldots 2$. Conveniently, these IM tones are near ω_A which is already being measured to determine the small-signal impedance. Just like conventional EIS, the measurement is repeated at various values of ω_A until the relevant frequency range has been spanned.

II. Methods

Because our eventual goal is to build a multiplexed impedance biosensor, we use a microfabricated 6×6 array of individually addressable $300\,\mu$m square gold electrodes on a glass microchip. A custom-built socket mounted on the underside of a printed circuit board (PCB) provides electrical contact with measurement electronics, and a hole through the PCB allows access to the electrodes. An O-ring between the socket and the microchip prevents liquid from leaking away from the electrodes. As shown in Fig. 1, a two-tone excitation voltage is applied to one electrode at a time (the DUT) and the resulting current is measured. Electrodes are sequentially connected to the measurement electronics using an analog mux. LabView coordinates the process and extracts the tone amplitudes.

To improve precision, we use a two-channel ratiometric scheme; the reference channel contains a fixed impedance in place of the DUT. Both signals are amplified and acquired by the same ADC; their ratio yields the DUT impedance after correction using a technique adapted from [8]. This technique uses the measurement data from three known impedances to eliminate systematic errors arising from unmodeled components of Z_f (e.g. stray capacitance), crosstalk between channels (e.g. sampling residue), and the fixed time difference in sampling instants. The coefficients α_1 and α_2 are computed from ratios of the fundamental and IM tone amplitudes. These are averaged for each upper-lower tone pair for each fundamental tone after normalization by the measured $Z_f(\omega)$ and $Z_0(\omega)$.

All data is fit to a circuit model consisting of a resistor in series with a constant phase element (CPE), which represent

[1]In our case the nonlinearity is capacitive and thus factors of $\frac{1}{2}$ and $\frac{1}{3}$ in the first and second IM tones have been included to reflect charge conservation for nonlinear capacitors [7].

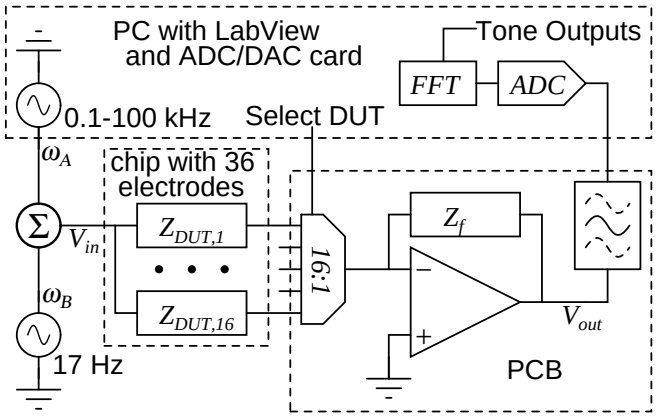

Fig. 1. A simplified system diagram of the measurement circuit. The combination of low frequency and high frequency excitation across nonlinear Z_{DUT} creates IM tones adjacent to the main high frequency tone. The main tone is used to determine the small-signal impedance Z_0 and the IM tones give nonlinear terms α_1 and α_2 according to Eq. 5.

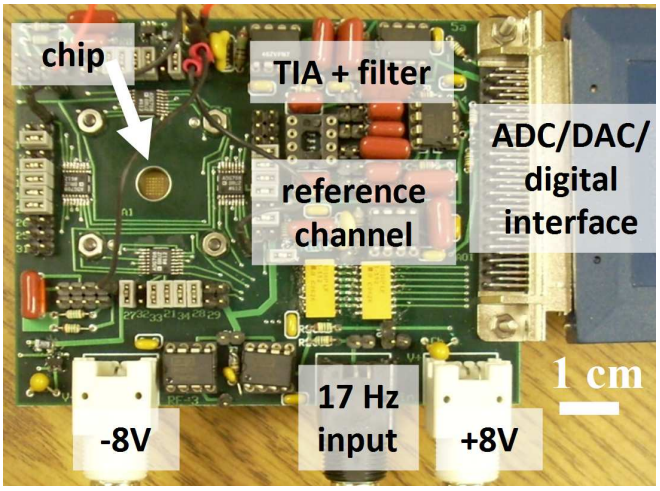

Fig. 2. Our custom EIS + nonlinearity measurement system implemented on a 4"x3" PCB. The 36-electrode chip is held beneath the PCB and can be seen through the hole where the buffer solution is added.

the solution resistance and electrode-solution capacitance [2]. The typical measured impedance for our system is $R_{sol} = 1\,\text{k}\Omega$ in series with $Z_{CPE} = (14\,\text{"nF"})^{-1}(j\omega)^{-0.92}$ ($\simeq 7\,$nF at 1 kHz). Acquisition begins at least 50 ms after the excitation signal is applied to ensure steady state is reached ($\text{RC} < 30\,\mu$s) and continues for 1 second at each frequency step. For results presented here, the small-signal tone (ω_A) has 2 mV amplitude (swept from 100 Hz to 100 kHz in 13 steps) and the larger, slower tone (ω_B) is 17 Hz with 50 mV amplitude. The measurement buffer is PBS (10 mM phosphate buffer pH 7.4, 138 mM NaCl, 2.7 mM KCl). After initial impedance measurements, a small amount of biological target is injected and post-binding measurements are taken.

The excitation signal is applied via a Ag/AgCl electrode inserted into the buffer from above (not shown in Fig. 2). Because the solution contains a fixed concentration of Cl^-, the contact has a reproducible built-in potential which we take as a reference (+81 mV vs. Ag/AgCl/sat. KCl). A two-

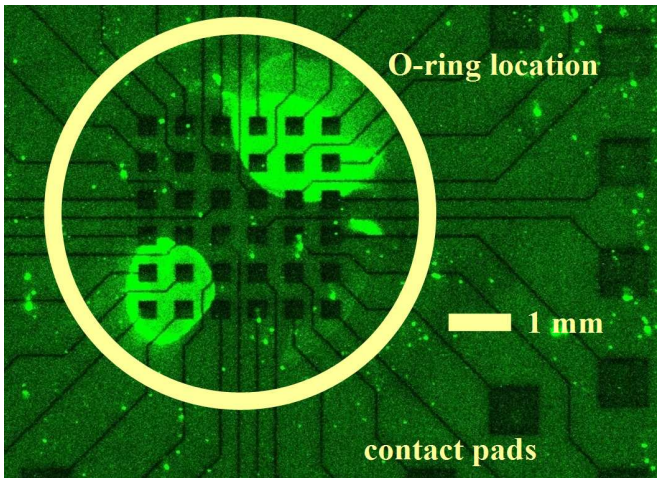

Fig. 3. Fluorescent micrograph of chip showing FITC-labeled target binding in two corners as desired. Because of backside illumination, the gold electrodes and traces areas appear dark. Some of the contact pads are visible and the location of the O-ring is indicated.

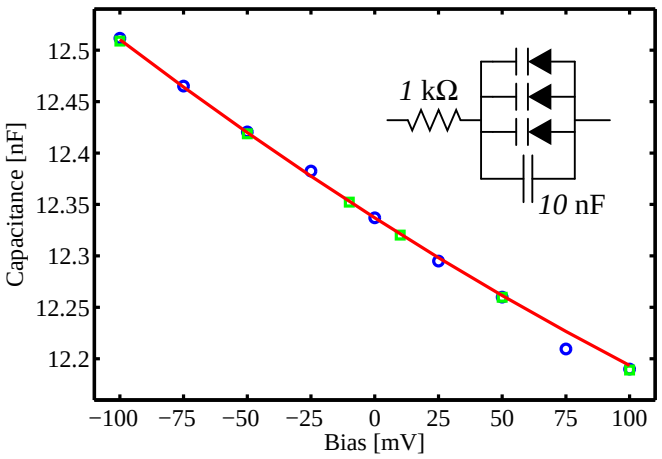

Fig. 4. Measured capacitance vs. bias for the DUT shown in the inset. The solid curve is predicted from the measurement of Z_0, α_1, and α_2 at 0 mV bias. The circles are the Z_0 values measured by our apparatus with applied DC bias, and the squares are measured with a commercial LCR meter.

electrode measurement is possible because the reference electrode can supply the required current and the solution resistance is small [3].

For the proof-of-principle experiments presented here, biotin is the probe and avidin is the target. The target is pre-labeled with a fluorophore so that probe-target binding can easily be verified (Fig. 3). Here we briefly describe the probe immobilization process. Thin layers of poly(L-lysine) and poly(acrylic acid) are formed, followed by NHS/EDC treatment to form amine-reactive sites. Protein probes (BSA-biotin and BSA) are spotted and attach covalently. To quench remaining amine-reactive sites, a dilute solution of BSA is applied followed by washing in PBS. Chips are stored for up to a week at 4 °C and soaked in PBS before use. Probes are hand-spotted in each corner region, and 4 electrodes per corner are electrically characterized. For future work, each of the 36 electrodes could be functionalized with a unique probe and all electrodes could be measured simultaneously using a multichannel acquisition system.

III. Results

To characterize the performance of our measurement system, we used varactors to create a non-biological DUT with bias-dependent impedance. The impedance was measured using the same method as the biofunctionalized electrodes. As expected, the extracted series resistance and CPE phase parameter were 1.00 kΩ and 1.00, respectively. As can be seen in Fig. 4, the nonlinearity measurements obtained at 0 mV bias at 1 kHz were sufficient to predict the bias-dependent capacitance within 0.1%. Our measurements agree with those of a commercial LCR meter.

At frequencies $\ll 15$ kHz the dominant contributor to the electrode-electrolyte impedance is the CPE representing the electrode-solution capacitance. The measured CPE can be thought of as a series combination of the ionic double-layer capacitance and the capacitance of the probe layer [9]. The double-layer capacitance exhibits voltage dependence as introduced in Section I. The Gouy-Chapman theory predicts a double-layer capacitance of about 84 nF for our electrodes in PBS. Thus at 1 kHz, roughly 8% of the applied voltage drops across the ionic double-layer and the remainder appears across the biofunctionalized interface. As $\alpha_2 \simeq 188\,\mathrm{V}^{-2}$ for the double-layer capacitance model in Eq. 1, we expect to measure $\alpha_2 \simeq 14\,\mathrm{V}^{-2}$ but observed only about half of that. We attribute this result to the crude double-layer model used in the foregoing calculation; in reality one contribution of the ionic capacitance is independent of bias voltage (predicted by the Stern modification of the Gouy-Chapman theory [3]) which will reduce the nonlinearity.

The ionic double-layer capacitance contribution is minimized at the PZC, or the applied potential at which the surface is charge neutral (see Eq. 1). Fig. 5 shows that the DC bias exhibiting minimum capacitance shifts upon target binding, suggesting that the net surface charge changes. In fact, the probe surface (BSA, pI ~ 5) is negatively charged and the target (avidin, pI ~ 10) is positively charged. We conclude that the observed changes in nonlinearity probably depend at least partly on changing surface charge, which modulates the voltage-dependent double layer capacitance. Thus, detecting target binding via nonlinearity may be somewhat akin to field-effect biosensors, which detect surface charge by other means [10].

A multitude of investigators have used impedance changes to detect probe-target binding [2]. Data shown in Fig. 6 demonstrate that changes in nonlinearity can also be used to indicate target binding; α_1 increases for binding ($n=4$) and decreases or remains constant if there is no binding ($n=8$). This agrees with the trend observed in Fig. 5 in which the putative PZC shifts.

Because there is no redox species present in our experiments (the measured parallel resistance is > 50 MΩ), the interface capacitance is the origin of the observed nonlinearity. For faradaic processes, the potential-dependent redox

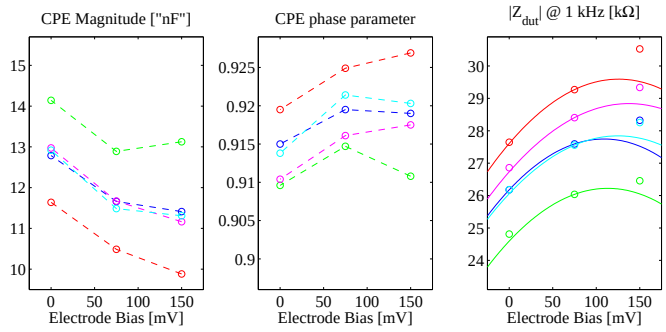

(a) Before target addition

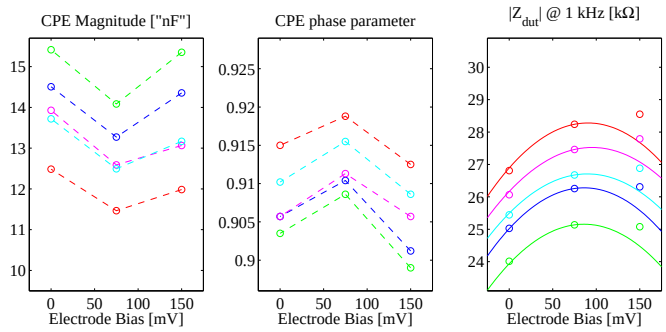

(b) After target addition

Fig. 5. Measured CPE magnitude, CPE phase, and impedance at 1 kHz from multiple electrodes on a single chip before and after introduction of $1\,\mu g/mL$ avidin. Measurements were taken at 0 mV, 75 mV, and 150 mV bias. The solid lines show the impedance values extrapolated from the nonlinear terms at 75 mV and the open circles show the measured values; the inaccuracy stems from changes in the CPE phase between these bias points. Note that the minimum CPE value (or maximum impedance) shifts to less positive potentials upon target addition. Interestingly, the CPE phase also depends on DC bias, with maximum at maximum impedance. The total impedance increases with decreased CPE value and with decreased CPE phase; the balance of these factors results in a monotonic impedance vs. bias in our data.

reaction is strongly nonlinear [11], implying that this measurement approach could be even more useful for faradaic biosensors. In fact, it has been shown that using large excitation signals in faradaic single-frequency AC voltammetry can speed determination of electrochemical variables [12].

For all measurements we observed $|\alpha_1|$ values in the range of 0.1–$1\,V^{-1}$ and $|\alpha_2|$ values in the range of 2–$10\,V^{-2}$, satisfying the assumptions used in deriving Eq. 5.

IV. Conclusions

A two-tone excitation allows the measurement of the impedance nonlinearity concurrently with the small-signal impedance. Applied to impedance biosensors, this method can either reduce the total measurement time in cases where bias dependence is explicitly measured (e.g. [5]) or else provide information about bias dependence that can be useful in discerning probe-target binding (e.g. detect surface charge). We demonstrate that protein binding could be discriminated on the basis of nonlinearity changes alone.

This two-tone measurement approach can be used in any impedance-measurement application in which nonlinearity or bias dependence is of interest. Though at present it requires

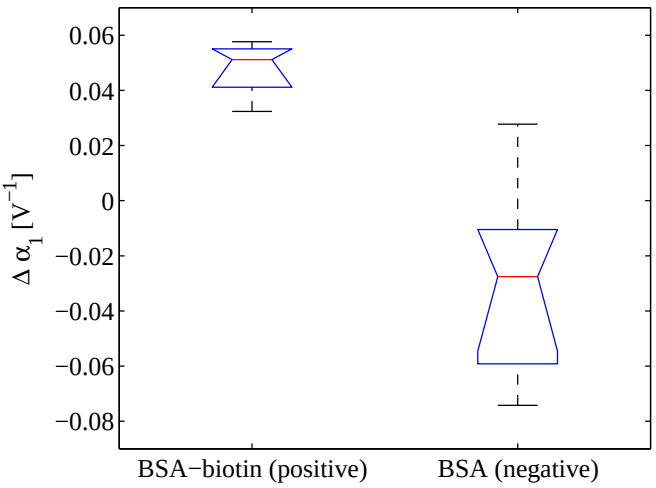

Fig. 6. Box plot demonstrating that changes in measured nonlinearity value α_1 can indicate target binding. The notch indicates the 95% confidence interval. These measurements are from various electrodes from a single chip measured at 0 mV bias after exposure to $250\,ng/mL$ avidin for 1 minute.

semi-custom apparatus, such functionality could be incorporated into future commercial instruments. The physical causes of impedance nonlinearity in biological interfaces is an interesting research area. Measuring nonlinearity may prove a fruitful tool in the ongoing efforts to improve the performance of electrical biosensors.

References

[1] E. Katz and I. Willner, "Probing biomolecular interactions at conductive and semiconductive surfaces by impedance spectroscopy: Routes to impedimetric immunosensors, dna-sensors, and enzyme biosensors," *Electroanalysis*, vol. 15, no. 11, p. 913, 2003.

[2] J. S. Daniels and N. Pourmand, "Label-free impedance biosensors: Opportunities and challenges," *Electroanalysis*, vol. 19, no. 12, p. 1239, 2007.

[3] A. J. Bard and L. R. Faulkner, *Electrochemical Methods: Fundamentals and Applications*, 2nd ed. New York: Wiley, 2001.

[4] G. Barbero, A. L. Alexe-Ionescu, and I. Lelidis, "Significance of small voltage in impedance spectroscopy measurements on electrolytic cells," *Journal of Applied Physics*, vol. 98, no. 11, p. 113703, 2005.

[5] M. L. O'Grady and K. K. Parker, "Dynamic control of protein-protein interactions," *Langmuir*, vol. 24, no. 1, p. 316, 2008.

[6] S. Nakata, N. Kido, M. Hayashi, M. Hara, H. Sasabe, T. Sugawara, and T. Matsuda, "Chemisorption of proteins and their thiol derivatives onto gold surfaces: Characterization based on electrochemical nonlinearity," *Biophysical Chemistry*, vol. 62, no. 1-3, p. 63, 1996.

[7] K. Kundert, "Modeling varactors," *www.designers-guide.org*, 2002.

[8] J. Schroder, S. Doerner, T. Schneider, and P. Hauptmann, "Analogue and digital sensor interfaces for impedance spectroscopy," *Measurement Science & Technology*, vol. 15, no. 7, p. 1271, 2004.

[9] R. P. Janek, W. R. Fawcett, and A. Ulman, "Impedance spectroscopy of self-assembled monolayers on au(111): evidence for complex double-layer structure in aqueous naclosub 4 at the potential of zero charge," *Journal of Physical Chemistry B*, vol. 101, no. 42, p. 8550, 1997.

[10] P. Bergveld, "Thirty years of isfetology: What happened in the past 30 years and what may happen in the next 30 years," *Sensors and Actuators, B: Chemical*, vol. 88, no. 1, p. 1, 2003.

[11] A. Richardot and E. T. McAdams, "Harmonic analysis of low-frequency bioelectrode behavior," *IEEE Transactions on Medical Imaging*, vol. 21, no. 6, p. 604, 2002.

[12] A. A. Sher, A. M. Bond, D. J. Gavaghan, K. Harriman, S. W. Feldberg, M. W. Duffy, S. X. Guo, and J. Zhang, "Resistance, capacitance, and electrode kinetic effects in fourier-transformed large-amplitude sinusoidal voltammetry: Emergence of powerful and intuitively obvious tools for recognition of patterns of behavior," *Analytical Chemistry*, vol. 76, no. 21, p. 6214, 2004.